Immunity 25, 297–308, August 2006 ©2006 Elsevier Inc. DOI 10.1016/j.immuni.2006.06.012

Cytoskeletal Regulation Couples LFA-1 Conformational Changes to Receptor Lateral Mobility and Clustering

Christopher W. Cairo,[1] Rossen Mirchev,[1] and David E. Golan[1,2,*]
[1] Department of Biological Chemistry and Molecular Pharmacology
Harvard Medical School
250 Longwood Avenue
Boston, Massachusetts 02115
[2] Hematology Division
Brigham and Women's Hospital
75 Francis Street
Boston, Massachusetts 02115

Summary

The $\alpha_L\beta_2$ integrin (leukocyte function-associated antigen-1 [LFA-1]) is regulated to engage and maintain T cell adhesion. Conformational changes in the receptor are associated with changes in receptor-ligand affinity and are necessary for firm adhesion. Less well understood is the relationship between receptor conformation and the regulation of its lateral mobility. We have used fluorescence photobleaching recovery and single-particle tracking to measure the lateral mobility of specific conformations of LFA-1. These measurements show that different receptor conformations have distinct diffusion profiles and that these profiles vary according to the activation state of the cell. Notably, a high-affinity conformation of LFA-1 is mobile on resting cells but immobile on phorbol-12-myristate-13-acetate-activated cells. This activation-induced immobilization is prevented by a calpain inhibitor and by an allosteric LFA-1 inhibitor. Our results suggest that current models of LFA-1 regulation are incomplete and that LFA-1 confinement by cytoskeletal attachment regulates cell adhesion both negatively and positively.

Introduction

The adhesion of T cells to their cellular partners is a tightly regulated and dynamic process. At various times, the T cell must adhere firmly to endothelial cells within the vasculature and to antigen-presenting cells in the lymph nodes and periphery. For each of these interactions, the primary adhesion molecule pair consists of T cell $\alpha_L\beta_2$ integrin (CD11a-CD18), known as leukocyte function-associated antigen-1 (LFA-1), and its ligand intercellular adhesion molecule-1 (ICAM-1).

A central question regarding the function of LFA-1 has been the relative importance of changes in receptor affinity versus receptor clustering upon cell activation (Carman and Springer, 2003; van Kooyk and Figdor, 2000). Changes in receptor conformation are known to be responsible for changes in receptor affinity (Shimaoka et al., 2003). Although the high-affinity forms of the integrin are necessary for adhesion (Lu et al., 2001b), both receptor and ligand must become engaged and aligned at the site of adhesion under physiological conditions (Dustin et al., 1997). Therefore, changes in LFA-1 lateral distribution must also be important for adhesion. Under certain conditions, artificially increased LFA-1 mobility can enhance adhesion (Kucik et al., 1996). In addition, LFA-1 has been shown to cluster after engagement of multivalent ligand (Kim et al., 2004).

The lateral mobility of membrane receptors, including integrins, is often regulated by interactions with cytoskeletally associated components (Liu et al., 2000). The mobility of the β_2 integrin has been shown to depend on both cytoskeletally associated proteins and the activation state of the cell (Geiger et al., 2000; Smith et al., 2005; Tadokoro et al., 2003; van Kooyk and Figdor, 2000). Studies of β_2 integrin mobility on resting cells have found that the receptor is confined by cytoskeletal attachment through the cytoplasmic tail of the receptor (Jin and Li, 2002). Activation of the cell by phorbol-12-myristate-13-acetate (PMA) or cytokine results in increased receptor lateral mobility (Constantin et al., 2000; Jin and Li, 2002; Kucik et al., 1996). These observations have supported the current paradigm of LFA-1 mobility regulation: the inactive receptor is maintained in a confined pool and then released when it is needed to mediate adhesion. Arguing against this simple model is the observation that ICAM-1-ligated LFA-1 is also confined by cytoskeletal attachment (Peters et al., 1999). Furthermore, related integrins become confined upon ligand binding (Felsenfeld et al., 1996).

The relationship between LFA-1 conformation and cytoskeletal attachment has not been explored in depth. Advances in the characterization of monoclonal antibodies (mAb) directed against specific conformations of LFA-1 allow direct investigation of the role of integrin conformation in receptor mobility, confinement, and adhesion. Many well-characterized epitopes for both inactive and active conformations have been identified, and antibodies have been used to observe conformational switching both in vitro and in vivo (Lu et al., 2001a; Ma et al., 2002; Shamri et al., 2005). Recent work has established that cell stimulation leads to a switch from the closed to the extended form of LFA-1 and that subsequent interaction with ligand results in additional conformational changes that mediate firm adhesion under shear (Shamri et al., 2005). Smith et al. have observed that cells treated with a mAb that stabilizes the high-affinity LFA-1 conformation have a decreased mobile fraction, although these receptors diffuse too slowly for their diffusion coefficient to be characterized by fluorescence photobleaching recovery (FPR) (Smith et al., 2005).

We sought to understand in detail the relationship between the conformational state of LFA-1 and the regulation of LFA-1 mobility. We measured the diffusion profiles of LFA-1 on live T cells via single-particle tracking (SPT), a technique with greater sensitivity than FPR for slowly diffusing receptors. We confirmed that different conformational states of LFA-1 manifest dramatic differences in lateral mobility. We showed that each

*Correspondence: dgolan@hms.harvard.edu

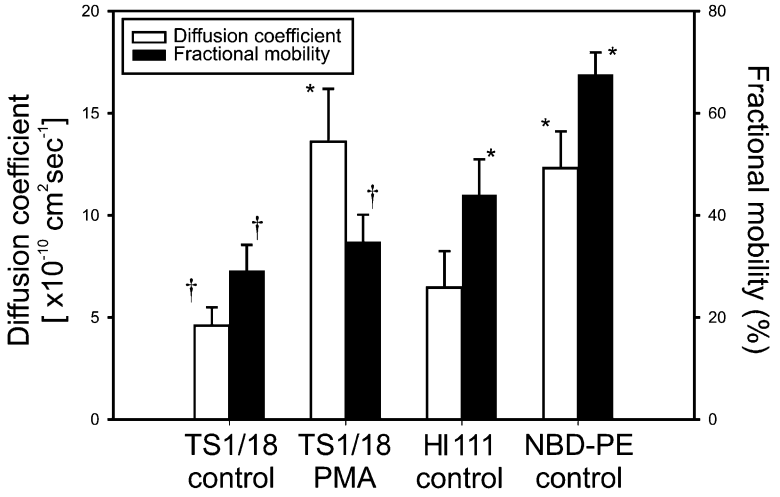

Figure 1. Lateral Mobility of LFA-1 Determined by FPR

The lateral mobility of LFA-1 was measured by FPR. Jurkat cells were labeled with FITC-derivatized anti-LFA-1 F(ab)' fragments under the following conditions: TS1/18 on resting (control) cells (n = 13 cells), TS1/18 on PMA-treated cells (n = 22), and HI111 on resting cells (n = 13). Resting cells were also labeled with a fluorescent lipid, NBD-PE, to determine the mobility of lipids in the plasma membrane (n = 23). Each point represents the results of at least two independent experiments. Error is shown as the standard error of the mean (SEM). (*$p < 0.01$, relative to TS1/18 on resting cells; †$p < 0.005$, relative to NBD-PE on resting cells.)

conformational state consists of multiple subpopulations with different rates of mobility and degrees of cytoskeletal attachment. The diffusion profiles of each conformational epitope also showed specific changes upon activation of the cell by PMA. Finally, we observed that the ligated form of LFA-1 has a unique diffusion profile, establishing the ability of the cell to recognize and respond to ligand-induced conformational changes. We propose that conformational changes in LFA-1 are coupled to receptor mobility, and thereby to receptor clustering, via cytoskeletal regulators.

Results

Activation of T Cells with PMA Induces Increased LFA-1 Mobility Measured by FPR

We used fluorescence photobleaching recovery (FPR) to characterize the average lateral mobility of two different LFA-1 epitopes on T cells (Figure 1). FITC-labeled F(ab)' fragments were used to eliminate potential cross-linking artifacts from bivalent IgG. The TS1/18 epitope is found on the I-like domain of the β_2 chain, and the antibody blocks adhesion but is not conformationally specific (Beals et al., 2001; Lu et al., 2001a). The HI111 epitope is found on the I-domain of the α_L chain; the antibody does not block adhesion, is specific for the closed conformation of the integrin, and is masked by activation (Ma et al., 2002). The lateral diffusion coefficients of these two epitopes on resting T cells were $4.6 \pm 0.9 \times 10^{-10}$ cm^2s^{-1} and $7 \pm 2 \times 10^{-10}$ cm^2s^{-1}, respectively. Both epitopes had large immobile fractions; fractional mobilities were 29% ± 5% and 44% ± 7%, respectively. Activation of cells with PMA increased the diffusion coefficient of TS1/18 to $14 \pm 3 \times 10^{-10}$ cm^2s^{-1} ($p < 0.01$), but there was no significant change in fractional mobility (35% ± 5%). We used the lateral mobility of a fluorescently labeled lipid, nitrobenzoxadiazole-phosphatidylethanolamine (NBD-PE), to define the upper limit of receptor mobility in the T cell membrane. NBD-PE had a diffusion coefficient of $12 \pm 2 \times 10^{-10}$ cm^2s^{-1} and fractional mobility of 68% ± 4% in this system. The fractional mobility of NBD-PE was significantly greater than that of LFA-1 in both resting and PMA-stimulated cells ($p < 0.05$).

These FPR measurements suggested that, as reported by others (Kim et al., 2004; Kucik et al., 1996), cell activation leads to increased diffusivity of the mobile fraction of LFA-1 molecules. Activation of the cell did not result in a significant change in the fractional mobility of LFA-1, suggesting that the majority of LFA-1 molecules are in a confined state both before and after cell activation. In addition, the fractional mobility of an LFA-1 conformation-dependent epitope, HI111, was significantly different from that of the conformationally nonspecific epitope TS1/18 ($p < 0.01$). In order to probe with finer resolution the relationship between LFA-1 conformation and lateral mobility, we turned to nonensemble techniques for quantifying the lateral mobility of LFA-1.

SPT of LFA-1 Epitope TS1/18 Reveals PMA Activation-Dependent Subpopulations

Single-particle tracking has been employed at 30 frames per second (FPS) to measure the lateral mobility of LFA-1 (epitopes IB4 and 2E6) on transformed B cells (Jin and Li, 2002; Kucik et al., 1996). These experiments revealed that cell activation causes a substantial increase in the diffusivity of LFA-1, in agreement with our FPR results. We reasoned that the increased sensitivity of SPT measurements for slowly diffusing molecules could resolve the identity of the immobile fraction of LFA-1 found in FPR experiments on T cells. Cells were labeled with antibody- or ligand-adsorbed beads, and trajectories of individual beads attached to LFA-1 were observed with high-speed video enhanced microscopy (Mirchev and Golan, 2001; Saxton and Jacobson, 1997). We used high-speed measurements over a short duration (1000 FPS over 4 s) to minimize contributions of cell motility to the observed trajectories. Trajectories were analyzed by fitting the mean-square displacement (MSD) curve according to standard methods (see Supplemental Data available with this article online) (Saxton and Jacobson, 1997). The MSD data could be analyzed to yield three parameters for each trajectory: D_{micro}, the diffusion coefficient over a short time interval (4 ms); D_{macro}, the time-dependent diffusion coefficient fit over a long time interval (1.5 s); and α, a parameter that describes the time dependence of the diffusion coefficient and indicates the mode of motion of the labeled molecule.

Table 1. Diffusion Parameters Determined by SPT

				Mean Values[a]			Subpopulations[b]			
Label	Cell	Treatment[c]	n	D_{micro}	D_{macro}	α	%	D_{mobile}	%	$D_{immobile}$
HI111	E6.1	untreated	70	9.0 ± 0.6	2.4 ± 0.4	0.7 ± 0.1	64	2.2 ± 0.4	36	0.15 ± 0.47
HI111	E6.1	cytoD	33	11 ± 0.8	4.5 ± 0.7	0.9 ± 0.1	82	4.1 ± 0.3	18	0.42 ± 0.62
TS1/18	E6.1	untreated	75	7.3 ± 0.5	1.8 ± 0.3	0.8 ± 0.1	28	4.7 ± 0.9	72	0.44 ± 0.55
TS1/18	E6.1	cytoD	36	7.8 ± 0.8	2.8 ± 0.6	1.0 ± 0.1	66	3.1 ± 0.5	34	0.31 ± 0.68
TS1/18	E6.1	PMA	39	8.2 ± 0.9	3.5 ± 0.7	0.9 ± 0.1	51	5.3 ± 0.9	49	0.72 ± 0.87
TS1/18	E6.1	lovastatin	42	8.3 ± 0.6	1.8 ± 0.3	0.7 ± 0.1	41	3.6 ± 0.8	59	0.37 ± 0.70
TS1/18	E6.1	PMA+lovastatin	42	7.3 ± 0.9	2.3 ± 0.4	0.8 ± 0.1	61	3.0 ± 1.5	39	0.11 ± 1.85
TS1/18	E6.1	PMA+cal-I	46	5.2 ± 0.8	1.6 ± 0.3	1.0 ± 0.1	39	3.0 ± 0.7	61	0.27 ± 0.53
TS1/18	PBL	untreated	40	3.3 ± 0.7	0.8 ± 0.4	1.3 ± 0.1	13	3.8 ± 1.9	87	0.14 ± 0.73
TS1/18	PBL	PMA	46	5.4 ± 0.6	0.6 ± 0.1	1.0 ± 0.1	33	1.3 ± 1.0	67	0.11 ± 0.71
MEM148	E6.1	untreated	39	8.2 ± 0.7	2.1 ± 0.4	0.7 ± 0.1	46	4.0 ± 1.7	54	0.32 ± 1.60
MEM148	E6.1	PMA	31	5.5 ± 1.1	1.4 ± 0.4	1.1 ± 0.1	30	4.4 ± 1.0	70	0.27 ± 0.67
MEM148	E6.1	lovastatin	45	8.1 ± 0.6	1.0 ± 0.2	0.5 ± 0.1	60	1.2 ± 0.7	40	0.13 ± 0.90
MEM148	E6.1	PMA+lovastatin	44	4.7 ± 0.7	1.6 ± 0.4	0.9 ± 0.1	47	2.5 ± 1.0	53	0.15 ± 1.00
MEM148	E6.1	PMA+cal-I	42	5.6 ± 0.7	1.5 ± 0.3	0.9 ± 0.1	46	2.2 ± 0.5	54	0.25 ± 0.44
MEM148	PBL	untreated	46	4.8 ± 0.6	0.9 ± 0.2	1.0 ± 0.1	49	1.5 ± 0.6	51	0.12 ± 0.55
MEM148	PBL	PMA	42	2.0 ± 0.5	0.11 ± 0.03	1.2 ± 0.1	7	0.9 ± 2.5	93	0.04 ± 0.70
ICAM-1	E6.1	untreated	38	6.6 ± 0.8	1.5 ± 0.3	0.9 ± 0.1	18	7.0 ± 1.2	82	0.52 ± 0.57
ICAM-1	E6.1	cytoD	48	8.5 ± 0.6	2.7 ± 0.4	0.8 ± 0.1	58	3.7 ± 0.4	42	0.43 ± 0.46
ICAM-1	E6.1	PMA	24	3.7 ± 0.8	1.3 ± 0.3	0.9 ± 0.1	<1	ND[d]	86	0.94 ± 0.24

[a] Values represent mean ± SEM. Units of D_{micro} and D_{macro} are 10^{-10} cm^2s^{-1}.
[b] Population analysis of D_{macro} values was used to determine the percentage of trajectories in the mobile and immobile ranges of the diffusion profile (see text for additional detail and Figure S4 for additional analysis).
[c] Conditions were: untreated (buffer + 0.1% DMSO), cytoD (1 μM in buffer + 0.1% DMSO), PMA (200 ng/mL in buffer + 0.1% DMSO), lovastatin (100 μM in buffer + 0.1% DMSO), PMA + lovastatin (200 ng/mL PMA, 100 μM lovastatin in buffer + 0.1% DMSO), PMA + cal-I (200 ng/mL PMA, 26 μM cal-I in buffer + 0.1% DMSO). Buffer was HBSSB. See Supplemental Data for additional analysis.
[d] See text for discussion of the immobile assignment of trajectories obtained for this condition.

The mean values of each of these parameters showed relatively small differences among the different LFA-1 epitopes on resting and activated cells (Table 1). As described below, however, subpopulation analysis of D_{macro} values showed that LFA-1 mobility varied markedly according to its molecular conformation and the activation state of the cell. Therefore, we focused our analysis on these subpopulations.

Analysis of LFA-1 D_{macro} data showed the presence of subpopulations for virtually all LFA-1 epitopes in resting and activated cells (Figure 2 and see below). We used a kernel density function to calculate a population density estimate and thereby determine the relative contributions of the component populations (see Supplemental Data, Section S5) (Sheather, 2004). In general, two subpopulations of LFA-1 trajectories could be distinguished by this analysis: a mobile population, with D_{macro} centered at values around 3.6×10^{-10} cm^2s^{-1}; and an immobile population, with D_{macro} centered at values around 0.3×10^{-10} cm^2s^{-1} (Figure S4). We refer to the overall population density as the LFA-1 diffusion profile for each set of conditions.

The major population of LFA-1 labeled by mAb TS1/18 was immobile, representing 72% of the diffusion profile at $D_{macro} = 0.4 \pm 0.6 \times 10^{-10}$ cm^2s^{-1} (Figure 2B). We used cytochalasin D (cytoD), which inhibits actin polymerization, to test the effect of disrupting cytoskeletal interactions on LFA-1 diffusion. Additionally, we used PMA to activate cells. Treatment with either cytoD or PMA caused an increase in the mobile population of LFA-1 (Figure 2C, 66% at $D_{macro} = 3.1 \pm 0.5 \times 10^{-10}$ cm^2s^{-1}; Figure 2D, 51% at $D_{macro} = 5.3 \pm 0.9 \times 10^{-10}$ cm^2s^{-1}). These results suggested that LFA-1 exists in at least two distinct populations on both resting and activated cells. A large fraction of LFA-1 appears to be maintained in the immobile state on resting cells (Figure 2E), and this reserve pool of receptors is released from cytoskeletal constraints upon cell activation. These observations are qualitatively consistent with previous reports of cytoD and PMA effects on integrin mobility and clustering, although we observed a larger mobile population of LFA-1 on resting Jurkat cells than has been observed on other cell types (Kim et al., 2004; Kucik et al., 1996).

SPT of Conformation-Dependent Epitopes HI111 and MEM148 Shows Divergent Shifts in Subpopulations

We employed two known conformation-dependent epitopes of LFA-1, HI111 and MEM148, to determine whether the diffusion profile of LFA-1 was dependent on molecular conformation. HI111 labels an inactive, closed conformation of LFA-1 (Ma et al., 2002), whereas MEM148 labels an active, open conformation of LFA-1 (Tan et al., 2001). The MEM148 epitope is found on the C-terminal region of the β_2 chain, and the antibody neither blocks adhesion nor activates the cell (Drbal et al., 2001; Tan et al., 2001).

Both HI111 and MEM148 showed diffusion profiles different from those of TS1/18 (Figure 3). In resting cells, the mobile population was large for both epitopes: for HI111, 64% at $D_{macro} = 2.2 \pm 0.4 \times 10^{-10}$ cm^2s^{-1}; for MEM148, 46% at $D_{macro} = 4 \pm 2 \times 10^{-10}$ cm^2s^{-1}. These data indicated that both the inactive, closed LFA-1 conformation labeled by HI111 and the active, open conformation labeled by MEM148 have larger mobile populations than TS1/18-labeled receptors on resting Jurkat

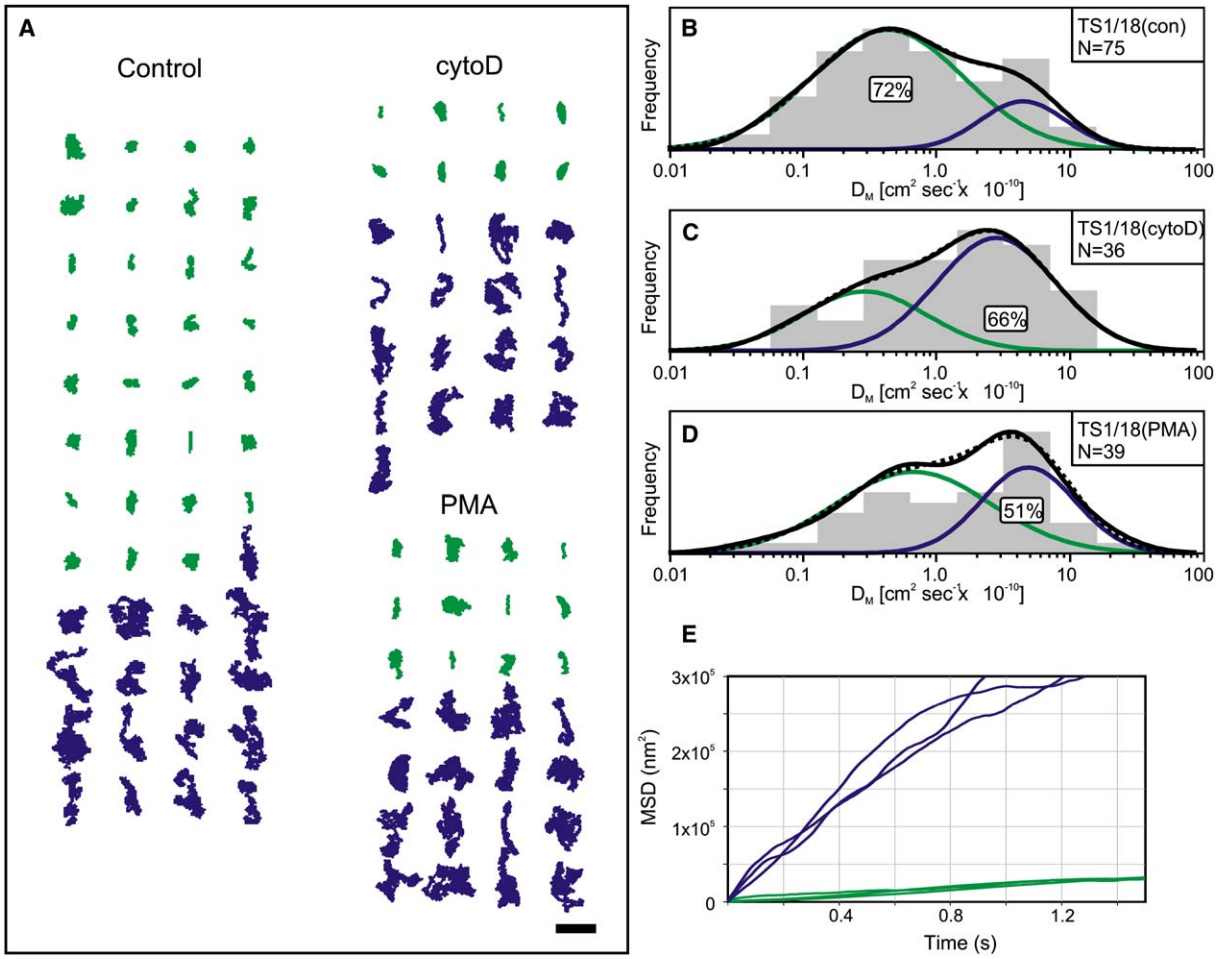

Figure 2. Single-Particle Tracking of LFA-1 Labeled with TS1/18

The diffusion of LFA-1 labeled with TS1/18 was observed with F(ab)'-coated beads and high-speed microscopy (see Experimental Procedures). (A) Representative trajectories (4 s, 1000 FPS) are shown for control cells in buffer containing DMSO (0.1%), cells treated with cytoD (1 μM, 0.1% DMSO), and cells treated with PMA (200 ng/mL, 0.1% DMSO). Representative trajectories are sorted by D_{macro} and colored according to the subpopulation in which they were classified: immobile (green) or mobile (blue). All trajectories are oriented such that the origin is toward the bottom of the figure and the terminus is toward the top of the figure. Scale bar represents 1 μm. Each condition represents the results of 2–4 independent experiments.

(B–D) The distribution of calculated diffusion constants (D_{macro}) is plotted as a histogram (gray) for each treatment: (B) control, (C) cytoD, (D) PMA. The population density is shown in black (solid line); the best fit of the population density is shown in black (dotted line) with the best-fitted subpopulations colored as in (A). The dominant subpopulation is indicated by a box that states the relative area of the peak. Complete peak fitting results are given in Table S2.

(E) The calculated MSD versus time interval is shown for three representative trajectories within each subpopulation, colored as in (A).

cells. In the case of HI111, treatment with cytoD caused an increase in both the fraction of mobile trajectories and their diffusivity (Figure 3B, 82% at $D_{macro} = 4.1 \pm 0.3 \times 10^{-10}$ cm^2s^{-1}). This observation suggested that the immobile fraction of receptors labeled by HI111 is tethered by cytoskeletal regulators on resting cells.

Interestingly, the effect of PMA on the diffusion profile of MEM148 was opposite to the effect of this cellular activator on the diffusion profile of TS1/18 (Figure 3E). The mobile population decreased from 46% to 30%, while the immobile population increased to 70% at $D_{macro} = 0.3 \pm 0.7 \times 10^{-10}$ cm^2s^{-1}. Furthermore, computation of weighted parameters for the immobile population showed a dramatic increase in the α value, from 0.6 ± 0.2 to 1.4 ± 0.1, and a decrease in the D_{micro} value, from $7 \pm 1 \times 10^{-10}$ cm^2s^{-1} to $2.3 \pm 0.7 \times 10^{-10}$ cm^2s^{-1} (see Table S2). These results suggested that PMA activation causes the active, open conformation labeled by MEM148 to become largely immobile and to experience directed motion. We also used FPR to confirm that the vast majority of MEM148-labeled receptors were laterally immobile on cells treated with PMA (data not shown).

SPT Shows that ICAM-1-Ligated LFA-1 Is Immobile on Both Resting and PMA-Activated Cells

We next considered the effects of LFA-1 binding to its native ligand, ICAM-1. The trajectories of LFA-1-ICAM-1 complexes on cells could be observed with the use of ICAM-1-labeled beads (Figure 4; Peters et al., 1999). We found that ICAM-1-ligated LFA-1 occupied primarily the immobile region of the diffusion profile (Figure 4A,

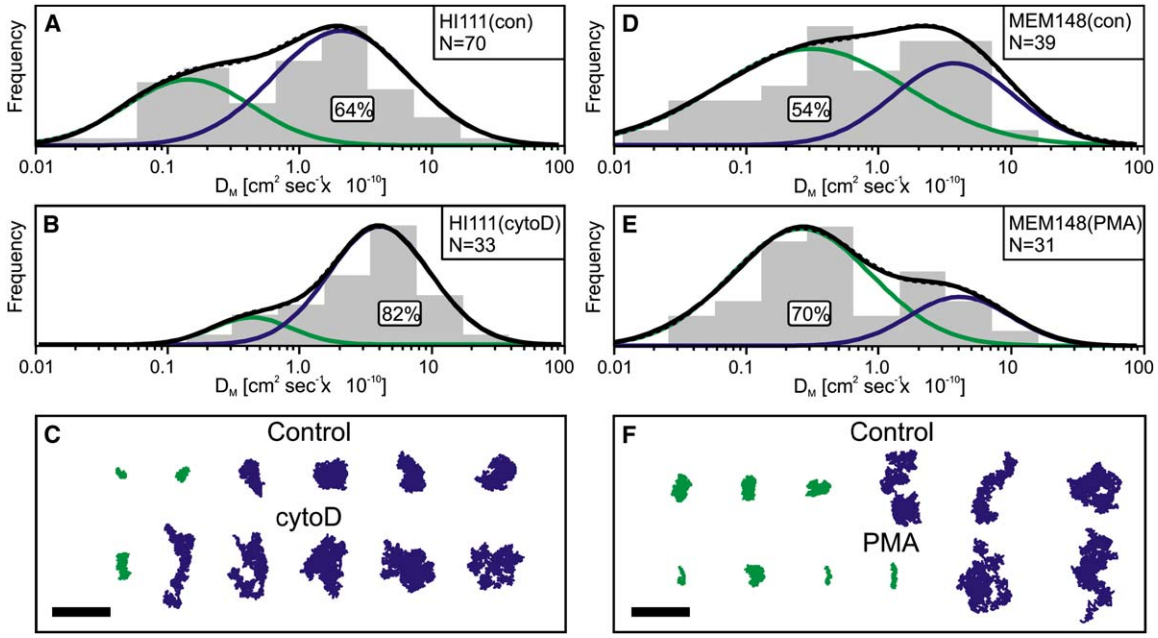

Figure 3. Single-Particle Tracking of Conformation-Dependent Epitopes HI111 and MEM148

The diffusion of LFA-1 labeled with HI111 (specific for the closed conformation of LFA-1) or MEM148 (specific for the open conformation of LFA-1) was observed with F(ab)'-coated beads and high-speed microscopy.

(A and B) Cells labeled with HI111 beads were treated with (A) control buffer containing DMSO (0.1%) or (B) cytoD (1 μM, 0.1% DMSO).

(C) Representative trajectories are shown for control cells (top) and cytoD-treated cells (bottom).

(D and E) Cells labeled with MEM148 beads were treated with (D) control buffer containing DMSO (0.1%) or (E) PMA (200 ng/mL, 0.1% DMSO).

(F) Representative trajectories are shown for control cells (top) and PMA-treated cells (bottom). Scale bar represents 1 μm. Each condition represents the results of 2–4 independent experiments.

Population and trajectory data are plotted as described in the legend to Figure 2. The epitope recognized by HI111 is masked upon activation with PMA; therefore, it could not be labeled or observed on PMA-treated cells.

82% at D_{macro} = 0.5 ± 0.6 × 10^{-10} cm^2s^{-1}). Treatment with cytoD caused an increase in the mobile population (Figure 4B, 58% at D_{macro} = 3.7 ± 0.4 × 10^{-10} cm^2s^{-1}), showing that the immobile population was sensitive to cytoskeletal disruption. On PMA-treated cells, ICAM-1-ligated LFA-1 trajectories were centered in an intermediate region of the diffusion profile (Figure 4C, 86% at D_{macro} = 0.9 ± 0.2 × 10^{-10} cm^2s^{-1}). Therefore, assignment of this population as "mobile" or "immobile" was difficult (see Figure S4). However, the weighted D_{micro} value for this population was reduced from 14 ± 1 × 10^{-10} cm^2s^{-1} in untreated cells to 3.1 ± 0.6 × 10^{-10} cm^2s^{-1} in PMA-treated cells. Together with the relatively low D_{macro} value, the D_{micro} value that was more consistent with an immobile population (see Table S2) suggested that this peak should be considered immobile, most likely due to cytoskeletal attachment of LFA-1 upon ICAM-1 ligation. This interpretation was also consistent with biochemical, biophysical, and functional evidence in the literature (Dustin et al., 2004; Peters et al., 1999).

A Conformational Inhibitor Alters the Diffusion Profile of LFA-1

Several small molecule inhibitors are known to interfere with LFA-1-ICAM-1 interactions. Lovastatin is the archetypal "L-site" inhibitor (also called the I-domain allosteric site inhibitor); this drug induces a conformational change in the I-domain of LFA-1, preventing adoption of the active I-domain conformation required for ligand binding (Kallen et al., 1999; Weitz-Schmidt et al., 2004; Welzenbach et al., 2002). We tested whether the conformational change caused by this inhibitor would alter the LFA-1 diffusion profile (Figure 5).

Compared to untreated cells (Figure 2B), lovastatin-treated cells showed an increase in the mobile population observed with TS1/18 (Figure 5A, 41% at D_{macro} = 3.6 ± 0.8 × 10^{-10} cm^2s^{-1}). Lovastatin had a similar effect in PMA-activated cells, such that the primary LFA-1 population was laterally mobile (Figure 5B, 61% at D_{macro} = 3 ± 2 × 10^{-10} cm^2s^{-1}; compare to Figure 2D). Lovastatin-treated cells observed with MEM148 also showed an increase in the mobile population (Figure 5E, 60% at D_{macro} = 1.2 ± 0.7 × 10^{-10} cm^2s^{-1}) compared to untreated cells (Figure 3D, 46% at D_{macro} = 4 ± 2 × 10^{-10} cm^2s^{-1}). This mobile population was largely maintained in PMA-activated cells treated with lovastatin (Figure 5F, 47% at D_{macro} = 3 ± 1 × 10^{-10} cm^2s^{-1}). The latter result suggested that lovastatin inhibits the activation-induced conformational change in LFA-1 required to restrict the diffusion of the mobile population (compare Figure 5F to Figure 3E).

A Calpain Inhibitor Alters LFA-1 Mobility

Talin is a central regulator of cellular adhesion dynamics and a putative regulator of LFA-1 (Smith et al., 2005; Stewart et al., 1998). The regulatory function of talin is mediated by calpain, which cleaves the talin head

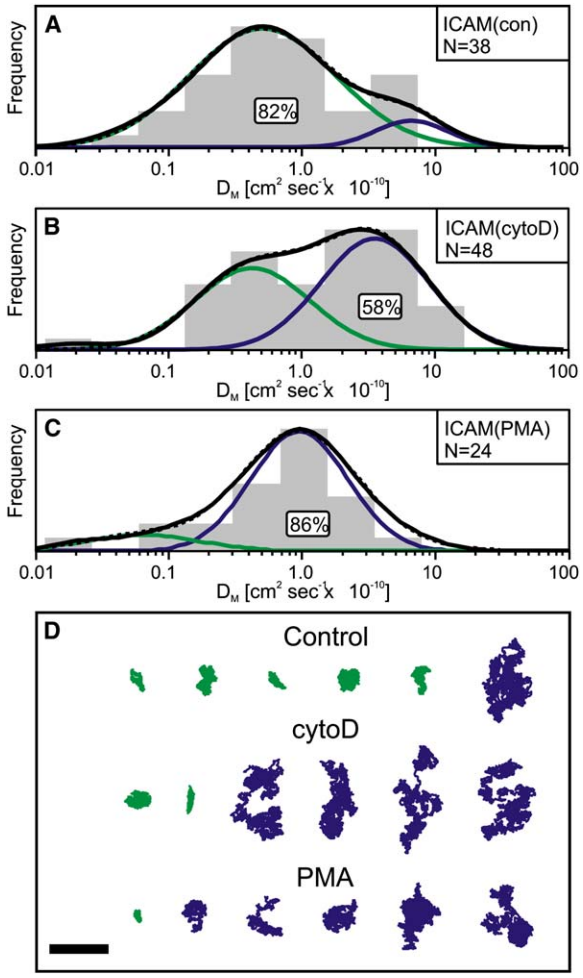

Figure 4. Single-Particle Tracking of ICAM-1-LFA-1 Adhesion Complex

(A–C) The diffusion of ICAM-1-LFA-1 complexes was observed by SPT with ICAM-1-labeled beads. Cells were treated with buffer containing: (A) DMSO (0.1%), (B) cytoD (1 μM, 0.1% DMSO), or (C) PMA (200 ng/mL, 0.1% DMSO).

(D) Representative trajectories are shown for control (top), cytoD-treated (middle), and PMA-treated (bottom) cells. Scale bar represents 1 μm. Each condition represents the results of 2–4 independent experiments.

Population and trajectory data are plotted as described in the legend to Figure 2.

domain from its cytoskeletal attachment site (Franco et al., 2004). We tested the involvement of calpain activity in LFA-1 mobility regulation by examining the effect of calpain inhibitor I (cal-I) on activation-induced changes in the lateral mobility of LFA-1 (Figure 5). We reasoned that calpain inhibition might attenuate the cytoskeletal release of TS1/18-labeled LFA-1 in cells treated with PMA. Indeed, upon PMA stimulation, TS1/18-labeled LFA-1 showed a smaller mobile population in cal-I-treated cells (Figure 5C, 39% at D_{macro} = 3.0 ± 0.7 × 10^{-10} cm^2s^{-1}) than in untreated cells (Figure 2D, 51% at D_{macro} = 5.3 ± 0.9 × 10^{-10} cm^2s^{-1}). We also tested for the involvement of calpain proteolysis in the activation-induced immobilization of MEM148-labeled LFA-1. We found that cal-I treatment maintained the large mobile population of LFA-1 (Figure 5G, 46% at D_{macro} = 2.2 ± 0.5 × 10^{-10} cm^2s^{-1}) that was lost upon PMA stimulation (Figure 3E, 30% at D_{macro} = 4 ± 1 × 10^{-10} cm^2s^{-1}). Together, these inhibition studies supported a key role for calpain activity in the PMA-stimulated cytoskeletal regulation of LFA-1.

Lateral Mobility of LFA-1 Is Reduced on PBL Compared to Jurkat, but Shows Similar Changes upon PMA Activation

To ascertain whether our observations of LFA-1 mobility regulation in Jurkat were specific to this transformed cell line, we repeated our key experiments in peripheral blood lymphocytes (PBL) (Figure 6). We used both the TS1/18 and MEM148 labels to measure LFA-1 mobility on resting and PMA-stimulated PBL. For both labels, LFA-1 manifested relatively slow diffusion (D_{macro} = 0.1–0.9 × 10^{-10} cm^2s^{-1}) in resting PBL compared to Jurkat cells, but the immobile and mobile populations were still well resolved (see Figure S4). Each label showed the same regulation profile on PBL as on Jurkat: TS1/18 was immobile on resting cells (Figure 6A, 87% at D_{macro} = 0.1 ± 0.7 × 10^{-10} cm^2s^{-1}) and was partially released upon cell activation (Figure 6B, 33% at D_{macro} = 1 ± 1 × 10^{-10} cm^2s^{-1}), whereas MEM148 showed a large mobile population on resting cells (Figure 6C, 49% at D_{macro} = 1.5 ± 0.6 × 10^{-10} cm^2s^{-1}) and an absence of mobile molecules on activated cells (Figures 6D and 6E). Although the magnitudes of the population shifts and diffusion coefficients were different in the two cell types, both PBL and Jurkat responded to PMA stimulation by releasing TS1/18-labeled LFA-1 and immobilizing MEM148-labeled LFA-1.

Model of LFA-1 Regulation

Based on the diffusion profiles of LFA-1 populations labeled by HI111, MEM148, TS1/18, and ICAM-1, we propose a model of LFA-1 regulation that has at least four conformational states (Figure 6F). The inactive (closed) conformation labeled by HI111 is primarily mobile. The active (open) conformation labeled by MEM148 is also primarily mobile on resting cells, but is immobilized by cytoskeletal attachment when the cell is activated. The TS1/18 epitope is not conformationally specific, and its use is intended to provide an indication of the conformational milieu of all LFA-1 receptors. However, because both HI111 and MEM148 epitopes are primarily mobile on resting cells, the primarily confined TS1/18 profile must represent more than the sum of these two populations. Additionally, the contrary population shift between TS1/18 and MEM148 observed upon PMA treatment supports the existence of a third (intermediate) conformational state. The ICAM-1-ligated receptor is primarily immobile on resting cells and becomes almost totally immobile upon PMA treatment. This unique profile likely signifies the presence of a fourth, ligand-induced conformational state.

We speculate that the T cell could effectively control the activity of LFA-1 by altering the equilibria among mobile and cytoskeletally confined receptor pools. From our observations, it appears that LFA-1 is regularly found in multiple mobility states under any given set of conditions. We propose that the system can be considered as a set of chemical equilibria involving at least four

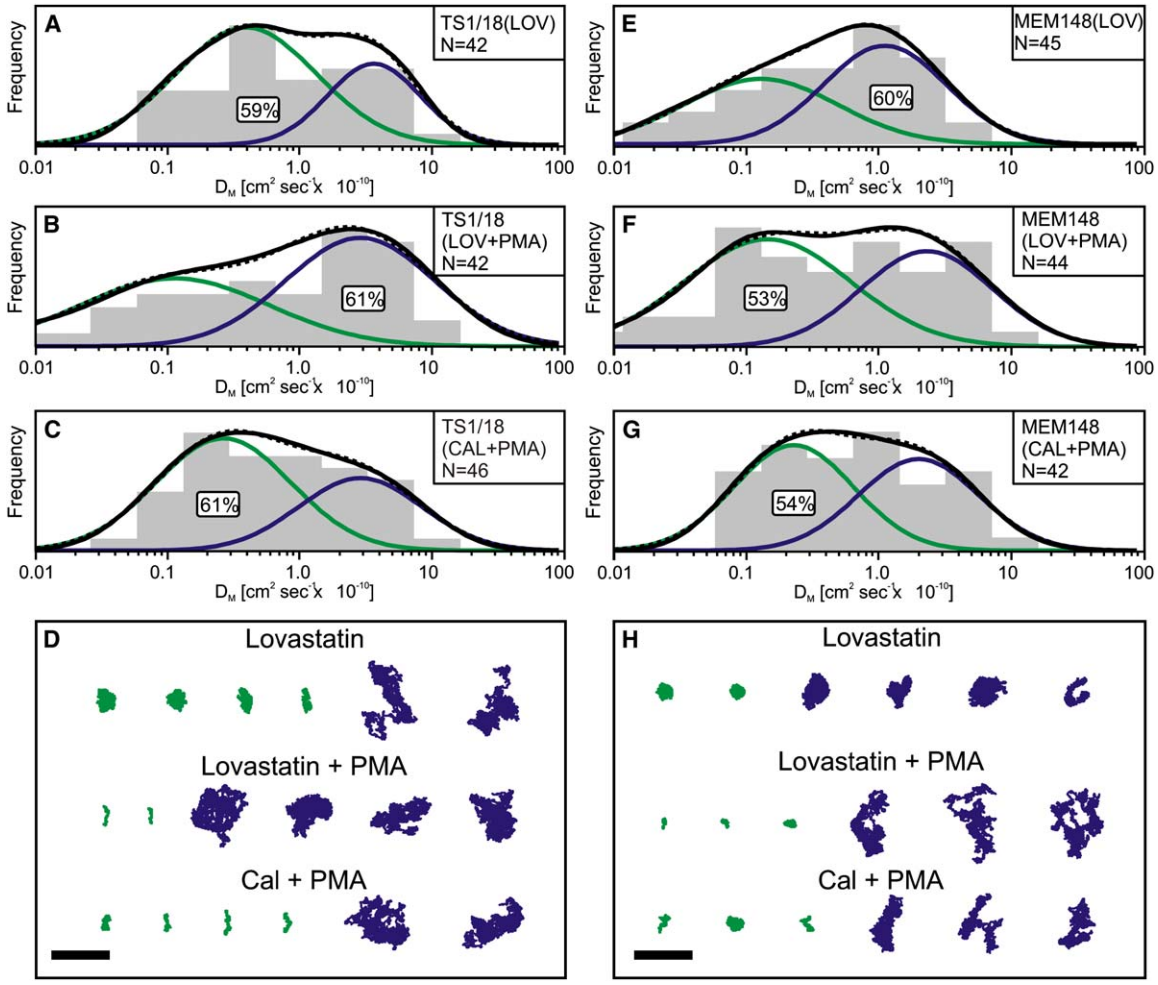

Figure 5. Single-Particle Tracking on Inhibitor-Treated Cells

The diffusion of LFA-1 labeled with TS1/18 or MEM148 was observed by SPT in the presence of lovastatin or calpain inhibitor I.

(A–C) Cells labeled with TS1/18 beads were treated with buffer containing: (A) lovastatin (100 μM, 0.1% DMSO), (B) lovastatin and PMA (200 ng/mL), or (C) calpain inhibitor I (26 μM, 0.1% DMSO) and PMA (200 ng/mL).

(D) Representative trajectories are shown for each condition.

(E–G) Cells labeled with MEM148 beads were treated with buffer containing: (E) lovastatin (100 μM, 0.1% DMSO), (F) lovastatin and PMA (200 ng/mL), (G) calpain inhibitor I (26 μM, 0.1% DMSO) and PMA (200 ng/mL).

(H) Representative trajectories are shown for each condition. Scale bar represents 1 μm. Each condition represents the results of 2–4 independent experiments.

Population and trajectory data are plotted as described in the legend to Figure 2.

conformational states of the receptor in mobile and cytoskeletally attached forms. In this model, the T cell could control LFA-1 activity by altering the mobile population of the relevant conformational state, and thereby control receptor clustering. Additionally, outside-in and inside-out signaling mechanisms could positively or negatively regulate LFA-1 activity by altering the equilibria among the various conformational states. As one example, these complex equilibria could be regulated by the site-specific phosphorylation of LFA-1 (Fagerholm et al., 2005). The differences we observe between PBL and Jurkat cells could be caused by variations in the expression of one or more cytoskeletal regulators, resulting in a perturbation of the equilibrium that alters the cytoskeletally attached population of LFA-1.

Discussion

Our results establish that each conformational state of LFA-1 has a characteristic diffusion profile in the plasma membrane of the T cell. In brief, it appears that cell activation mobilizes the intermediate conformation of LFA-1 in order to maximize receptor-ligand interactions, while cytoskeletal regulators preferentially immobilize the open and ligated conformations of LFA-1 in order to stabilize adhesion. The lateral mobility of LFA-1 is similarly regulated on Jurkat cells and peripheral blood lymphocytes, although the magnitudes of the population shifts and diffusion coefficients are different between the two cell types. Our results are consistent with a mass-action model of LFA-1 accumulation at sites of adhesion

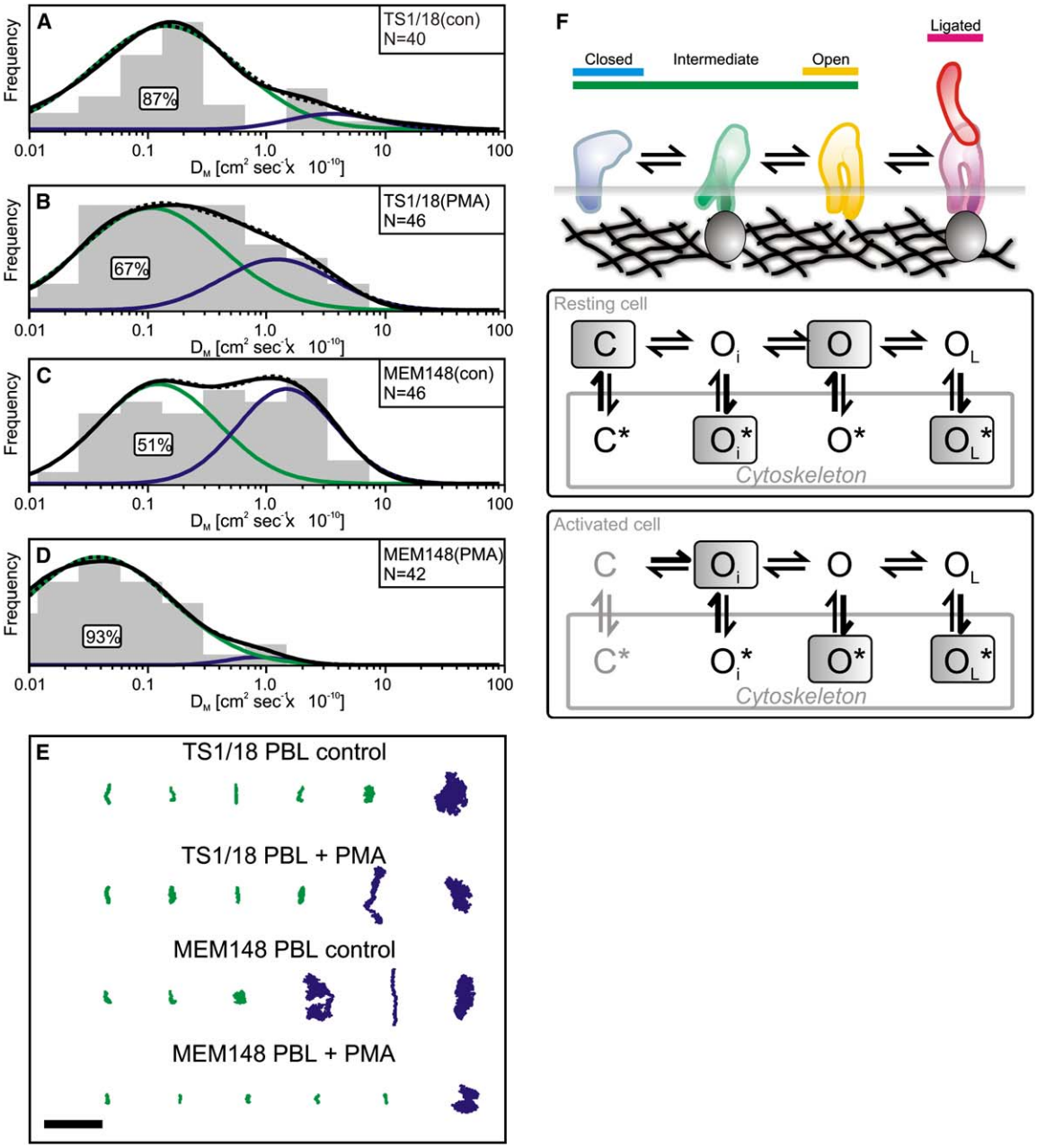

Figure 6. Diffusion of LFA-1 on Peripheral Blood Lymphocytes

Trajectories of TS1/18- or MEM148-labeled beads were observed on resting or PMA-treated PBL.

(A and B) Cells labeled with TS1/18 beads were treated with buffer containing: (A) DMSO (0.1%) or (B) PMA (200 ng/mL, 0.1% DMSO).

(C and D) Cells labeled with MEM148 beads were treated with buffer containing: (C) DMSO (0.1%) or (D) PMA (200 ng/mL, 0.1% DMSO).

(E) Representative trajectories are shown for each condition. Scale bar represents 1 μm. Each condition represents the results of three independent experiments.

Population and trajectory data are plotted as described in the legend to Figure 2.

(F) Based on our observations, we propose a model for the regulation of LFA-1 lateral diffusion on T cells. Top: The mAbs and ligand used in SPT and FPR experiments label specific LFA-1 conformations: HI111 labels the closed conformation (blue), TS1/18 labels an intermediate conformation (green) in addition to the closed and open forms, MEM148 labels the open conformation (yellow), and ICAM-1 induces the ligated conformation (red). Middle: The conformations of LFA-1 can be considered within a set of chemical equilibria in which receptor conformation and lateral mobility are variable. LFA-1 confinement by cytoskeletal attachment is denoted by an asterisk. On the resting cell, the closed conformation (C) of LFA-1 exists primarily as freely diffusing receptors. An intermediate conformation (O_i*) is primarily confined by cytoskeletal attachment, possibly through interactions with talin. The open conformation (O) of the receptor is primarily mobile on resting cells. Bottom: Cell activation releases the confinement of the intermediate conformation via calpain activity to produce a primarily mobile population (O_i). In contrast, receptors in the open conformation are confined by cytoskeletal attachment (O*). In both resting and activated cells, ICAM-1-ligated LFA-1 is largely confined by cytoskeletal attachment after ligation induces the bound conformation of the receptor (O_L*).

(Dustin et al., 2004; Kim et al., 2004) and with the notion that immobilization of ligated LFA-1 through cytoskeletal attachment may be critical in physiological settings (Shamri et al., 2005). Importantly, our results also suggest that the conformational state and lateral mobility of LFA-1 are coupled in order to provide regulation of receptor function on lymphocytes.

Although previous reports have examined the lateral mobility of LFA-1 via SPT (Kucik et al., 1996; Peters et al., 1999) and FPR (Gaborski et al., 2005; Kim et al., 2004; Smith et al., 2005), we describe here a set of experiments that characterizes directly the mobility of multiple conformational epitopes of LFA-1. Under virtually all conditions, we observe the presence of at least two distinct populations of LFA-1: a mobile population and an immobile population. Deconvolution of the populations according to D_{macro} values reveals much more substantial changes in LFA-1 mobility than the average values measured for the population as a whole. Therefore, for each set of conditions, we have analyzed the relative proportions of the mobile and immobile populations within the diffusion profile.

Previous models of LFA-1 regulation have proposed that the molecule is confined on resting cells and is released from its cytoskeletal constraints upon cell activation, resulting in increased mobility. Our results suggest a more complex and subtle regulation of LFA-1 mobility, in which the closed conformation is mobile on resting cells and the ligated conformation is confined on activated cells. We also conclude that interactions with cytoskeletally attached components are responsible, at least in part, for the slow diffusion of the immobile populations of all LFA-1 conformations. These populations are sensitive to treatment with cytoD and have smaller microdiffusion coefficients than the mobile populations, suggesting that the immobile molecules are tethered to the cytoskeleton.

The diffusion profiles of LFA-1 show evidence of both inside-out and outside-in signaling. Inside-out stimulation of the cell by PMA causes a large increase in the mobile population of LFA-1 that is labeled by TS1/18. Cell activation also substantially alters the diffusion profiles of the activation epitope, MEM148, and of ICAM-1-ligated LFA-1. Outside-in signaling is suggested by the observation that the various conformational epitopes of LFA-1 demonstrate markedly different diffusion profiles on both resting and PMA-activated cells, consistent with the propagation of conformational information from the ectodomains of LFA-1 to cytoskeletal regulators of the receptor.

The LFA-1 diffusion profile is modified by an allosteric inhibitor of I-domain conformational changes. Lovastatin is a well-characterized L-site inhibitor that binds to LFA-1 and prevents the I-domain and I-like domain conformational changes that are required for ICAM-1 binding (Welzenbach et al., 2002). When LFA-1 mobility is observed by TS1/18 epitope labeling, lovastatin treatment results in an increase in the mobile population on both resting and PMA-stimulated cells. Similarly, lovastatin increases the mobile population of the activation epitope MEM148 on resting cells. Importantly, lovastatin prevents the loss of the mobile population of MEM148-labeled LFA-1 upon PMA activation. This result suggests that the conformational change induced by the inhibitor mimics the open conformation labeled by MEM148, allowing the receptor to retain its laterally mobile character. Thus, effects on receptor lateral mobility could represent a substantial component of the mechanism by which allosteric inhibitors regulate LFA-1 function.

We used an inhibitor of calpain activity to confirm that calpain is one of the cytoskeletal regulators of LFA-1 (Franco et al., 2004; Stewart et al., 1998). A likely target of calpain is the cytoskeletally associated protein talin, which is known to anchor integrins including LFA-1 (Franco et al., 2004; Schoenwaelder et al., 1997; Schoenwaelder and Burridge, 1999; Stewart et al., 1998). In Jurkat cells, we found evidence that calpain cleavage is responsible for releasing the immobile pool of LFA-1 upon PMA stimulation. Our results also suggested that calpain activity is necessary for immobilizing the active conformation of LFA-1, implying that calpain cleavage of a regulatory protein is upstream of the immobilization interaction. For example, the cleavage of talin by calpain could be necessary to allow a downstream cytoskeletal regulator to recognize and immobilize the active conformation of LFA-1, perhaps by recognition of a shared binding site.

We compared the lateral mobility of LFA-1 on Jurkat cells to that on PBL and found that the profile of mobility regulation was similar on the two cell types. The diffusion coefficient of LFA-1 on PBL was lower than that on Jurkat under all conditions, and the magnitude of response to cell activation was altered. Nonetheless, the similarity in the direction of response suggests that similar cytoskeletal regulators are involved in the two cell types. Our finding that the mobile fraction of LFA-1 is larger on Jurkat cells than on PBL may help to explain the increased adhesion manifested by transformed LFA-1-expressing cells (Sigal et al., 2000). The specific mechanisms responsible for these changes may be relevant for neoplastic phenotypes that are associated with altered LFA-1 regulation (Tanaka, 1999).

In summary, we have observed the diffusion of LFA-1 on live T cells by a combination of ensemble (FPR) and nonensemble (SPT) methods. We find that conformational epitopes of the receptor have distinct diffusion profiles that are altered by cell activation. Our observations are consistent with a mass-action model of LFA-1 accumulation at sites of adhesion, and they provide a mechanism for adhesion strengthening. Additionally, we find evidence that allosteric inhibitors of LFA-1 stabilize a conformation of the receptor that has high mobility and is incapable of binding ligand (Weitz-Schmidt et al., 2001). Together, these results provide a new dynamic picture of LFA-1 regulation that couples receptor mobility and conformational change.

Our findings may also shed light on a continuing debate in the literature regarding the importance of changes in LFA-1 affinity versus clustering. Strong evidence has been found for the role of both mechanisms in LFA-1-mediated adhesion, and affinity and clustering are generally treated as separate mechanisms. While both mechanisms are necessary for adhesion (Kim et al., 2004; van Kooyk and Figdor, 2000), our data suggest that attempting to separate these two mechanistic concepts may be unwarranted. There is little doubt that LFA-1 conformational changes alter affinity of the

receptor (Shimaoka et al., 2001). By definition, changes in receptor clustering require alterations in receptor mobility (Klemm et al., 1998). Our results suggest that the mobility of LFA-1 is controlled by recognition of its conformational state by cytoskeletally attached proteins. In turn, conformational states of the receptor are regulated by both outside-in and inside-out signaling mechanisms (Kim et al., 2003; Porter et al., 2002). We propose that each conformational state of the receptor experiences a specific diffusion profile, which then controls the clustering of that receptor state. In this way, receptor affinity and mobility (Dustin et al., 1996, 2001) are both optimized for interaction with the intended multivalent ligand (Gestwicki et al., 2002; Kiessling et al., 2006), and receptor affinity state (conformation) and mobility (clustering) are integrated through the specific recognition of integrin conformation by cytoskeletal regulators.

Experimental Procedures

Antibodies and Reagents

Antibodies were purchased as mouse IgG and then digested and purified as F(ab)' fragments according to standard procedures. TS1/18 antibody against β_2 integrin (CD18) was purchased from Pierce Biotechnology (Rockford, IL), and clone MEM-148 was purchased from Serotec Ltd. (Kidlington, Oxford, UK). HI111 antibody against α_L integrin (CD11a) was purchased from BD Biosciences (San Diego, CA). Recombinant human ICAM-1 was purchased from R&D Systems, Inc. (Minneapolis, MN). NBD-PE was purchased from Avanti Polar Lipids (Alabaster, AL). Cytochalasin D and PMA were purchased from EMD Biosciences (San Diego, CA). Isotype control mouse IgG, calpain inhibitor I, Accuspin System-Histopaque 1077, and buffer reagents were purchased from Sigma-Aldrich, Inc. (St. Louis, MO); cell media and buffers were purchased from Invitrogen, Inc. (Carlsbad, CA).

Cells

Jurkat cells, clone E6.1, were obtained from ATCC (Manassas, VA) and grown in RPMI media supplemented with 10% fetal bovine serum and penicillin/streptomycin (1000 U/mL). Cells were harvested from cultures in exponential growth and washed three times with Hank's balanced salt solution (HBSS) supplemented with 1% (m/v) BSA (HBSSB). The cells were then resuspended in HBSSB containing either DMSO alone (0.1% v/v) or DMSO with PMA (200 ng/mL), cytoD (5 μg/mL), lovastatin (100 μM), or calpain inhibitor I (26 μM). Aliquots of the cell suspension (0.25 mL) were incubated for 30 min at 37°C and labeled with polystyrene microspheres for another 15 min at 37°C. The samples were then diluted to 1 ml with HBSSB and transferred to a 24-well plate containing 12 mm circular coverslips treated with cell-tak (BD Pharmingen). The plate was centrifuged at ~500 RPM for 7 min and then the wells were carefully washed seven times with fresh HBSSB (1 mL). The coverslip was then transferred to a microslide, seated with a thin circle of vacuum grease, and sealed with Cytoseal 60 (Richard-Allan Scientific, Kalamazoo, MI). Samples were observed experimentally within 90 min of sealing.

Peripheral blood lymphocytes (PBL) were isolated from normal whole blood by centrifugation with Histopaque 1077. Blood obtained from individual donors (2–3 mL) was centrifuged according to the manufacturer's protocol. Mononuclear cells at the interface were removed and washed three times with HBSS (4 mL). Cells were then incubated in RPMI 1640 containing 10% autologous plasma and penicillin/streptomycin (1000 U/mL) for 24 hr. Nonadherent cells were then used for experiments within 12 hr. All PBL experiments were replicated with cells from at least three different donors.

Bead Labeling

1 μm polystyrene microspheres were obtained from Polysciences (2.6% m/v). The beads were diluted to a stock solution of 1.3% (m/v) in DI water with 0.1% NaN_3 and sonicated for 15 min before each use. Beads (10 μl of stock solution) were labeled by incubation with monoclonal F(ab)' fragments or ICAM-1 (0.1–10 μg) for 1 hr in 0.2 ml of borate buffer (100 mM borate, 1 mM EDTA, 0.1% NaN_3 [pH 8.5]) at a final bead concentration of 0.05% (m/v). In all cases, we used the minimum amount of protein required to achieve selective binding of beads to cells. Control beads were labeled with polyclonal F(ab)' or BSA under identical conditions. After adsorption of the protein to the beads, the samples were diluted to 1 ml with blocking buffer (10 mM HEPES, 140 mM NaCl, 1 mM EDTA, 2% dextran, 1% BSA, 0.1% NaN_3, 0.1 μg/mL PEG-compound [pH 7.4]) and incubated for 1 hr. The samples were then sonicated for 15 min and centrifuged at 5000 RPM for 7 min. The supernatant was aspirated to 0.1 ml final volume, resuspended, and sonicated for 15 min immediately before use. All labeled bead samples were used within 48 hr of preparation. Selectivity of binding was confirmed at the start of each experiment by manually counting the number of positively labeled cells in ~20 random fields. Samples were used for tracking experiments if the selectivity of bead binding was more than 4-fold greater than the isotype control. Bead binding was typically 0.4% of cells for control beads and 2% (5-fold selectivity) for ICAM-1- (0.1 μg), 4% (10-fold) for TS1/18- (1.0 μg), 3% (6-fold) for MEM-148- (1.0 μg), and 3% (6-fold) for HI111- (1.0 μg) labeled beads.

Single-Particle Tracking

Cells were observed on a Nikon TE2000-E microscope equipped with DIC optics, with a 60× oil objective with an oil condenser (NA = 1.4) (Mirchev and Golan, 2001). Images of a single bead on individual cells were captured at 1000 FPS with a Fastcam Super 10K camera (Photron USA, Inc., San Diego, CA). Video data were processed with Metamorph (Universal Imaging, Downington, PA) and converted to trajectories. Trajectory data were analyzed with mean square displacement (MSD) analysis (Saxton and Jacobson, 1997) implemented in a custom program written in Matlab (Mathworks, Inc., Natick, MA) (see Supplemental Data). Jurkat cells were nonmotile under the conditions used for these experiments, but some PBL showed evidence of motility. Cell motility did not affect the interpretation of SPT data collected on PBL (see Figure S3).

Fluorescence Photobleaching Recovery

Jurkat cells were collected in exponential growth, washed three times with HBSSB, and then incubated for 30 min at 37°C with HBBSB containing DMSO (0.1% v/v) or DMSO with PMA (200 ng/mL). Cells were then labeled for 15 min with FITC-conjugated F(ab)' fragments (20 μg/mL) and transferred to a 6-well plate containing fresh HBSSB and a BSA-coated coverslip. For lipid diffusion experiments, NBD-PE was added to the cell suspension (10 μg/mL) for 15 min. The plate was centrifuged at ~500 RPM for 7 min to settle cells onto the glass. The coverslip was then washed twice with fresh HBSSB, transferred to a microslide, and sealed with vacuum grease and Cytoseal. Samples were observed within 90 min of sealing. FPR experiments were conducted on a Meridian Ultima workstation (Okemos, MI), with a 40× objective (NA = 1.3). Fluorescence recovery was observed over a 50–200 s period after the photobleach, depending on the rate of recovery. All experiments were performed on at least two separate days, with two different samples per experiment.

Supplemental Data

Supplemental Data include two tables, four figures, and Supplemental Experimental Procedures and can be found with this article online at http://www.immunity.com/cgi/content/full/25/2/297/DC1/.

Acknowledgments

We thank Prof. Lloyd Klickstein for helpful discussions. C.W.C. was funded by an NIH NRSA Postdoctoral Fellowship (F32 GM067292) and an NIH Training Grant (T32 HL07623). D.E.G. acknowledges funding from NIH grants R37HL032854 and U54HL070819. C.W.C. and D.E.G. are grateful for support from the Alexander and Margaret Stewart Trust.

Received: August 4, 2005
Revised: May 19, 2006
Accepted: June 6, 2006
Published online: August 10, 2006

References

Beals, C.R., Edwards, A.C., Gottschalk, R.J., Kuijpers, T.W., and Staunton, D.E. (2001). CD18 activation epitopes induced by leukocyte activation. J. Immunol. *167*, 6113–6122.

Carman, C.V., and Springer, T.A. (2003). Integrin avidity regulation: are changes in affinity and conformation underemphasized? Curr. Opin. Cell Biol. *15*, 547–556.

Constantin, G., Majeed, M., Giagulli, C., Piccio, L., Kim, J.Y., Butcher, E.C., and Laudanna, C. (2000). Chemokines trigger immediate beta 2 integrin affinity and mobility changes: differential regulation and roles in lymphocyte arrest under flow. Immunity *13*, 759–769.

Drbal, K., Angelisova, P., Cerny, J., Hilgert, I., and Horejsi, V. (2001). A novel anti-CD18 mAb recognizes an activation-related epitope and induces a high-affinity conformation in leukocyte integrins. Immunobiology *203*, 687–698.

Dustin, M.L., Ferguson, L.M., Chan, P.Y., Springer, T.A., and Golan, D.E. (1996). Visualization of CD2 interaction with LFA-3 and determination of the two-dimensional dissociation constant for adhesion receptors in a contact area. J. Cell Biol. *132*, 465–474.

Dustin, M.L., Golan, D.E., Zhu, D.M., Miller, J.M., Meier, W., Davies, E.A., and van der Merwe, P.A. (1997). Low affinity interaction of human or rat T cell adhesion molecule CD2 with its ligand aligns adhering membranes to achieve high physiological affinity. J. Biol. Chem. *272*, 30889–30898.

Dustin, M.L., Bromley, S.K., Davis, M.M., and Zhu, C. (2001). Identification of self through two-dimensional chemistry and synapses. Annu. Rev. Cell Dev. Biol. *17*, 133–157.

Dustin, M.L., Bivona, T.G., and Philips, M.R. (2004). Membranes as messengers in T cell adhesion signaling. Nat. Immunol. *5*, 363–372.

Fagerholm, S.C., Hilden, T.J., Nurmi, S.M., and Gahmberg, C.G. (2005). Specific integrin alpha and beta chain phosphorylations regulate LFA-1 activation through affinity-dependent and -independent mechanisms. J. Cell Biol. *171*, 705–715.

Felsenfeld, D.P., Choquet, D., and Sheetz, M.P. (1996). Ligand binding regulates the directed movement of beta 1 integrins on fibroblasts. Nature *383*, 438–440.

Franco, S.J., Rodgers, M.A., Perrin, B.J., Han, J.W., Bennin, D.A., Critchley, D.R., and Huttenlocher, A. (2004). Calpain-mediated proteolysis of talin regulates adhesion dynamics. Nat. Cell Biol. *6*, 977–983.

Gaborski, T., Waugh, R.E., and McGrath, J.L. (2005). Differences in mobility and distribution of selectins and beta-2 integrins in resting and crawling neutrophils. Biophys. J. *88*, 588A.

Geiger, C., Nagel, W., Boehm, T., van Kooyk, Y., Figdor, C.G., Kremmer, E., Hogg, N., Zeitlmann, L., Dierks, H., Weber, K.S.C., and Kolanus, W. (2000). Cytohesin-1 regulates beta-2 integrin-mediated adhesion through both ARF-GEF function and interaction with LFA-1. EMBO J. *19*, 2525–2536.

Gestwicki, J.E., Cairo, C.W., Strong, L.E., Oetjen, K.A., and Kiessling, L.L. (2002). Influencing receptor-ligand binding mechanisms with multivalent ligand architecture. J. Am. Chem. Soc. *124*, 14922–14933.

Jin, T.Q., and Li, J.X. (2002). Dynamitin controls beta(2) integrin avidity by modulating cytoskeletal constraint on integrin molecules. J. Biol. Chem. *277*, 32963–32969.

Kallen, J., Welzenbach, K., Ramage, P., Geyl, D., Kriwacki, R., Legge, G., Cottens, S., Weitz-Schmidt, G., and Hommel, U. (1999). Structural basis for LFA-1 inhibition upon lovastatin binding to the CD11a I-domain. J. Mol. Biol. *292*, 1–9.

Kiessling, L.L., Gestwicki, J.E., and Strong, L.E. (2006). Synthetic multivalent ligands as probes of signal transduction. Angew. Chem. Int. Ed. Engl. *45*, 2348–2368.

Kim, M., Carman, C.V., and Springer, T.A. (2003). Bidirectional transmembrane signaling by cytoplasmic domain separation in integrins. Science *301*, 1720–1725.

Kim, M., Carman, C.V., Yang, W., Salas, A., and Springer, T.A. (2004). The primacy of affinity over clustering in regulation of adhesiveness of the integrin alpha(L)beta 2. J. Cell Biol. *167*, 1241–1253.

Klemm, J.D., Schreiber, S.L., and Crabtree, G.R. (1998). Dimerization as a regulatory mechanism in signal transduction. Annu. Rev. Immunol. *16*, 569–592.

Kucik, D.F., Dustin, M.L., Miller, J.M., and Brown, E.J. (1996). Adhesion-activating phorbol ester increases the mobility of leukocyte integrin LFA-1 in cultured lymphocytes. J. Clin. Invest. *97*, 2139–2144.

Liu, S.C., Calderwood, D.A., and Ginsberg, M.H. (2000). Integrin cytoplasmic domain-binding proteins. J. Cell Sci. *113*, 3563–3571.

Lu, C.F., Ferzly, M., Takagi, J., and Springer, T.A. (2001a). Epitope mapping of antibodies to the C-terminal region of the integrin beta(2) subunit reveals regions that become exposed upon receptor activation. J. Immunol. *166*, 5629–5637.

Lu, C.F., Shimaoka, M., Zang, Q., Takagi, J., and Springer, T.A. (2001b). Locking in alternate conformations of the integrin alpha L beta 2 I domain with disulfide bonds reveals functional relationships among integrin domains. Proc. Natl. Acad. Sci. USA *98*, 2393–2398.

Ma, Q., Shimaoka, M., Lu, C., Jing, H., Carman, C.V., and Springer, T.A. (2002). Activation-induced conformational changes in the I domain region of lymphocyte function-associated antigen 1. J. Biol. Chem. *277*, 10638–10641.

Mirchev, R., and Golan, D.E. (2001). Single-particle tracking and laser optical tweezers studies of the dynamics of individual protein molecules in membranes of intact human and mouse red cells. Blood Cells Mol. Dis. *27*, 143–147.

Peters, I.M., van Kooyk, Y., van Vliet, S.J., De Grooth, B.G., Figdor, C.G., and Greve, J. (1999). 3D single-particle tracking and optical trap measurements on adhesion proteins. Cytometry *36*, 189–194.

Porter, J.C., Bracke, M., Smith, A., Davies, D., and Hogg, N. (2002). Signaling through integrin LFA-1 leads to filamentous actin polymerization and remodeling, resulting in enhanced T cell adhesion. J. Immunol. *168*, 6330–6335.

Saxton, M.J., and Jacobson, K. (1997). Single-particle tracking: applications to membrane dynamics. Annu. Rev. Biophys. Biomol. Struct. *26*, 373–399.

Schoenwaelder, S.M., and Burridge, K. (1999). Bidirectional signaling between the cytoskeleton and integrins. Curr. Opin. Cell Biol. *11*, 274–286.

Schoenwaelder, S.M., Yuan, Y.P., Cooray, P., Salem, H.H., and Jackson, S.P. (1997). Calpain cleavage of focal adhesion proteins regulates the cytoskeletal attachment of integrin alpha(IIb)beta(3) (platelet glycoprotein IIb/IIIa) and the cellular retraction of fibrin clots. J. Biol. Chem. *272*, 1694–1702.

Shamri, R., Grabovsky, V., Gauguet, J.M., Feigelson, S., Manevich, E., Kolanus, W., Robinson, M.K., Staunton, D.E., von Andrian, U.H., and Alon, R. (2005). Lymphocyte arrest requires instantaneous induction of an extended LFA-1 conformation mediated by endothelium-bound chemokines. Nat. Immunol. *6*, 497–506.

Sheather, S.J. (2004). Density estimation. Stat. Sci. *19*, 588–597.

Shimaoka, M., Lu, C.F., Palframan, R.T., von Andrian, U.H., McCormack, A., Takagi, J., and Springer, T.A. (2001). Reversibly locking a protein fold in an active conformation with a disulfide bond: integrin alpha L I domains with high affinity and antagonist activity in vivo. Proc. Natl. Acad. Sci. USA *98*, 6009–6014.

Shimaoka, M., Xiao, T., Liu, J.H., Yang, Y.T., Dong, Y.C., Jun, C.D., McCormack, A., Zhang, R.G., Joachimiak, A., Takagi, J., et al. (2003). Structures of the alpha L I domain and its complex with ICAM-1 reveal a shape-shifting pathway for integrin regulation. Cell *112*, 99–111.

Sigal, A., Bleijs, D.A., Grabovsky, V., van Vliet, S.J., Dwir, O., Figdor, C.G., van Kooyk, Y., and Alon, R. (2000). The LFA-1 integrin supports rolling adhesions on ICAM-1 under physiological shear flow in a permissive cellular environment. J. Immunol. *165*, 442–452.

Smith, A., Carrasco, Y.R., Stanley, P., Kieffer, N., Batista, F.D., and Hogg, N. (2005). A talin-dependent LFA-1 focal zone is formed by rapidly migrating T lymphocytes. J. Cell Biol. *170*, 141–151.

Stewart, M.P., McDowall, A., and Hogg, N. (1998). LFA-1-mediated adhesion is regulated by cytoskeletal restraint and by a Ca2+-dependent protease, calpain. J. Cell Biol. *140*, 699–707.

Tadokoro, S., Shattil, S.J., Eto, K., Tai, V., Liddington, R.C., de Pereda, J.M., Ginsberg, M.H., and Calderwood, D.A. (2003). Talin

binding to integrin beta tails: a final common step in integrin activation. Science *302*, 103–106.

Tan, S.M., Robinson, M.K., Drbal, K., van Kooyk, Y., Shaw, J.M., and Law, S.K.A. (2001). The N-terminal region and the mid-region complex of the integrin beta(2) subunit. J. Biol. Chem. *276*, 36370–36376.

Tanaka, Y. (1999). Activation of leukocyte function-associated antigen-1 on adult T-cell leukemia cells. Leuk. Lymphoma *36*, 15–23.

van Kooyk, Y., and Figdor, C.G. (2000). Avidity regulation of integrins: the driving force in leukocyte adhesion. Curr. Opin. Cell Biol. *12*, 542–547.

Weitz-Schmidt, G., Welzenbach, K., Brinkmann, V., Kamata, T., Kallen, J., Bruns, C., Cottens, S., Takada, Y., and Hommel, U. (2001). Statins selectively inhibit leukocyte function antigen-1 by binding to a novel regulatory integrin site. Nat. Med. *7*, 687–692.

Weitz-Schmidt, G., Welzenbach, K., Dawson, J., and Kallen, J. (2004). Improved lymphocyte function-associated antigen-1 (LFA-1) inhibition by statin derivatives—molecular basis determined by X-ray analysis and monitoring of LFA-1 conformational changes in vitro and ex vivo. J. Biol. Chem. *279*, 46764–46771.

Welzenbach, K., Hommel, U., and Weitz-Schmidt, G. (2002). Small molecule inhibitors induce conformational changes in the I domain and the I-like domain of lymphocyte function-associated antigen-1—molecular insights into integrin inhibition. J. Biol. Chem. *277*, 10590–10598.